

MODELING THE SPECTRAL RESPONSE OF BRAGG GRATINGS WRITTEN IN PHOTONIC CRYSTAL FIBERS

George S. Kliros

Hellenic Air-Force Academy, Department of Aeronautical Sciences
 Division of Electronics, Electrical Power and Telecommunications Engineering
 Dekeleia Air-Force Base, Attica GR-1010, Greece
 gskliros@ieee.org

Abstract

The spectral response of photonic crystal fiber Bragg gratings (PCFG) are investigated theoretically using a full vectorial Fast Multipole Method combined with exact equations for the reflection response of the Bragg gratings. When the PCF air-holes are infiltrated with different fluids, a downward shift is observed in the power reflectivity spectra. Both relative Bragg shift and grating's bandwidth depend linearly on the effective refractive index which supports the potential use of PCFGs as liquid sensors as well as tunable filters. It is also shown that the sensitivity of PCFG is strongly influenced by the choice of the structural parameters of the photonic crystal fiber.

1. INTRODUCTION

Photonic Crystal Fibers (PCF) have recently gain a broad application in telecommunication industry as well as in the traditional sensor industry. Endlessly single mode operation, high optical nonlinearities, the freedom to engineer the chromatic dispersion and the ability to fill the cladding air holes with liquids or gases are only a few of the physical virtues that have allowed these fibers to shine in a variety of roles from fiber lasers to fiber sensors. On the other hand, as for conventional fibers, the use of Bragg gratings written in a PCF can significantly enhance the device performance in a variety of environmental, biomedical and aerospace applications.

In this paper, motivated by the recent interest in developing photonic crystal sensors [1-3], we present a numerical simulation of Bragg gratings written in a PCF, as it is shown in Fig.1, using a full-vectorial fast multimode method combined with the coupled-mode theory of gratings. The sensitivity of our device is investigated by observing the shift in Bragg resonance wavelength in the reflectivity spectrum as a function of the change in effective refractive index when the PCF-holes are infiltrated with different fluids.

2. DEVICE MODELING

2.1. COUPLED-MODE THEORY OF BRAGG GRATINGS

In order to calculate the characteristics of uniform PCF Bragg Gratings (BG), the coupled-mode theory is applied. The PCF-BGs is considered longitudinally invariant, while a perturbation is introduced in the core region according to the relation:

$$\epsilon_r(\mathbf{z}) = \epsilon_{rs} + D\epsilon_{rs}(\mathbf{z}) \square n_s^2 + 2n_s \delta n_{eff}(\mathbf{z}) \quad (1)$$

where n_s is the refractive index (RI) of pure silica with a wavelength dependence given by the Sellmeier's equation

$$n_s(\lambda) = \left(1 + \sum_{j=1}^3 A_j \frac{\lambda^2}{\lambda^2 - \lambda_j^2} \right)^{1/2} \quad (2)$$

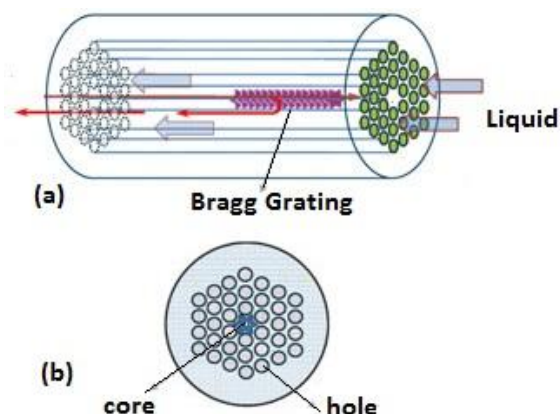


Figure 1. (a) Schematic of a photonic crystal fiber Bragg grating (b) Cross-section of the PCF.

where for A_j and λ_j are material constants with values: $A_1=0.6961663$, $A_2=0.4079426$, $A_3 = 0.8974794$, $\lambda_1=0.0684043$, $\lambda_2=0.116241$ and $\lambda_3 = 9.896161$.

For a uniform grating without chirp, the refractive index modulation can be written as

$$\delta n_{eff}(z) = \overline{\delta n_{eff}} \left[1 + v \cos\left(\frac{2\pi}{L_G} z\right) \right] \quad (3)$$

with $\overline{\delta n_{eff}}$ being the averaged refractive index change over one period, v is the fringe visibility of the index change, L_G is the period of the grating perturbation and z is the propagation distance.

In most uniform BG sensor application, only the reflection spectra of the BG are considered and the dominant interaction is between the forward propagating fundamental core mode and its counter propagating mode. Then, the system of coupled-mode equations has analytical solution [4] which leads to the following closed-form expression for the power reflection coefficient $r(L, \lambda)$ of a uniform fiber grating of length L .

$$r(L, \lambda) = \frac{\sinh^2\left(\sqrt{\kappa^2 - \hat{\sigma}^2} L\right)}{\cosh^2\left(\sqrt{\kappa^2 - \hat{\sigma}^2} L\right) - \frac{\hat{\sigma}^2}{\kappa^2}} \quad (4)$$

In Eq.(4), κ is the 'ac' coupling coefficient and $\hat{\sigma} = \sigma + \delta$ where σ is a generalized 'dc' self-coupling coefficient and the detuning parameter δ is defined as:

$$\delta \equiv \beta - \frac{\pi}{\Lambda_G} = 2\pi n_{eff} \left(\frac{1}{\lambda} - \frac{1}{\lambda_D} \right) \quad (5)$$

where λ_D is the design wavelength of the grating. For a single-mode reflection grating, the coupling parameters are given by the following simple relations:

$$\sigma = \frac{2\pi}{\lambda} \overline{\delta n_{eff}}, \quad \kappa = \frac{\pi v}{\lambda} \overline{\delta n_{eff}} \quad (6)$$

From Eq.(4), we find the maximum reflectivity for a Bragg grating is

$$r_{max} = \tanh^2(\kappa L) \quad (7)$$

which occurs at the 'Bragg wavelength'

$$\lambda_B = \left(1 + \frac{\overline{\delta n_{eff}}}{n_{eff}} \right) \lambda_D \quad (8)$$

A measurable bandwidth for the uniform Bragg grating is that between the first zeros on either side of the maximum reflectivity and is given by

$$\frac{D\lambda}{\lambda_D} = \frac{v \overline{\delta n_{eff}}}{n_{eff}} \sqrt{1 + \left(\frac{\lambda_D}{v \overline{\delta n_{eff}} L} \right)^2} \quad (9)$$

2.2. FAST MULTIPOLE METHOD

Multipole method (MPM) is a simulation method which is based on the principle of electromagnetic scattering properties for PCF. The method was first proposed by White and Kuhlmeier [5] for the simulation of PCF with circular holes. According to MPM the mode field is expanded by Fourier-Bessel function in the ℓ^{th} - hole, as

$$E_z = \sum_{m=-\infty}^{\infty} a_m^{(\ell)} J_m(k_{\perp}^i r_{\ell}) \exp(jm\varphi_{\ell}) \exp(j\beta z) \quad (11)$$

and in the adjacent medium of the circular ℓ^{th} - hole, the mode field is expanded as

$$E_z = \sum_{m=-\infty}^{\infty} \left[b_m^{(\ell)} J_m(k_{\perp}^s r_{\ell}) + c_m^{(\ell)} H_m(k_{\perp}^s r_{\ell}) \right] \times \exp(jm\varphi_{\ell}) \exp(j\beta z) \quad (12)$$

where

$$k_{\perp}^i = (k_0^2 n_i^2 - \beta^2)^{1/2}, \quad k_{\perp}^s = (k_0^2 n_s^2 - \beta^2)^{1/2} \quad (13)$$

n_i and n_s the refractive indexes of air and silica, respectively, $k_0=2\pi/\lambda$ is the free space wave-number and, β is the modal propagation constant. Magnetic field component H_z can be expressed by similar equations to Eqs. (11) and (12). We can obtain the relation between $a_m^{(\ell)}$, $b_m^{(\ell)}$, $c_m^{(\ell)}$ applying the electromagnetic field boundary conditions and then, the modal effective refractive index can be calculated as $n_{eff}=\beta/k_0$. Vector-based computations are employed instead of element-based ones using MATLAB technical language in order to reduce the computation time considerably.

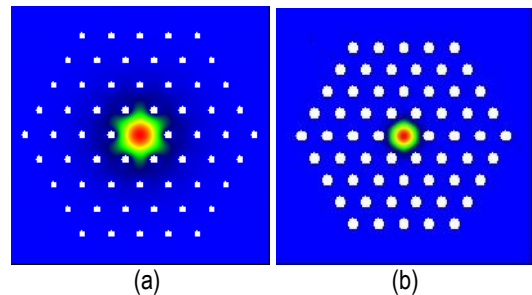


Figure 2. Energy flux distribution for the fundamental mode in PCF with air-holes of diameter a) $d/\Lambda=0.2$ and b) $d/\Lambda=0.4$ at the wavelength $\lambda=1.55 \mu\text{m}$.

3. RESULTS AND DISCUSSION

The PCF used to inscribe the Bragg grating has a structure with hexagonal symmetry with four layers of air-holes in the silica matrix and a missing hole in the center. The hole pitch is $\Lambda=2.3 \mu\text{m}$ and the ratio of hole diameter over pitch d/Λ is chosen to meet the condition of single-mode transmission. The structure of the PCF under study and the energy flux distribution of the fundamental mode calculated by MPM, for two different ratios $d/\Lambda=0.2$ and 0.4 , is depicted in Fig.2(a) and (b), respectively. It is clear from this figure that at larger ratios d/Λ the modes tends to be more confined in the core part of the structure. Furthermore, we consider the following parameters for the uniform grating written in the PCF-core: initial design wavelength $\lambda_D=1.55 \mu\text{m}$, refractive index modulation of $\delta n_{\text{eff}}=8.0 \times 10^{-4}$, visibility of the index change $v=0.02$ and grating length $L=70 \text{ mm}$.

In order to explore the spectral sensitivity of Bragg gratings written in the PCF, several fluids with refractive indexes varied from 1.25 (salol) to 1.40 (octane), are inserted into the holes. The effective RI of the guided fundamental mode in the PCF infiltrated by fluids, as a function of the operational wavelength, is calculated by MPM and the results are shown in Fig. 3. The red dots in Fig. 3 correspond to the effective refractive indexes at the design wavelength $\lambda_D=1.55 \mu\text{m}$.

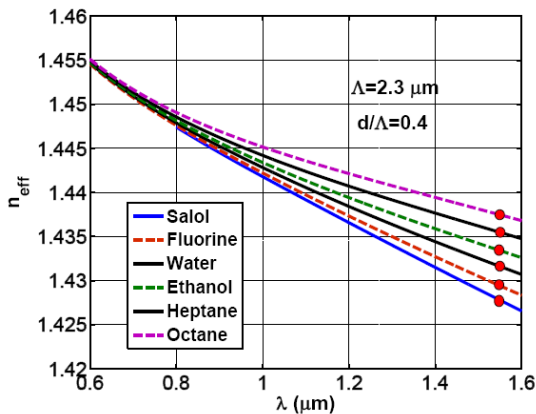


Figure 3. Energy flux distribution for the fundamental mode in PCF with air-holes of diameter a) $d/\Lambda=0.2$ and b) $d/\Lambda=0.4$ at the wavelength $\lambda=1.55 \mu\text{m}$.

Then, the power reflection spectra of the Bragg grating can be calculated using Eq.(4) as it is shown in Fig.4 for PCFs infiltrated by three different fluids.

The insertion of a fluid changes the cladding RI and modifies strongly the interaction between the

evanescent field of the guided mode and the medium in the holes. The effective index of the guided mode increases together with the RI of the holes. As a result, when a given fluid reaches the grating, the Bragg resonance experiences a downward shift, as depicted in Fig. 4. Additionally, it was found that the maximum reflectivities are almost the same. The Bragg wavelength λ_B at which the maximum reflectivity occurs can be calculated by Eq.(8).

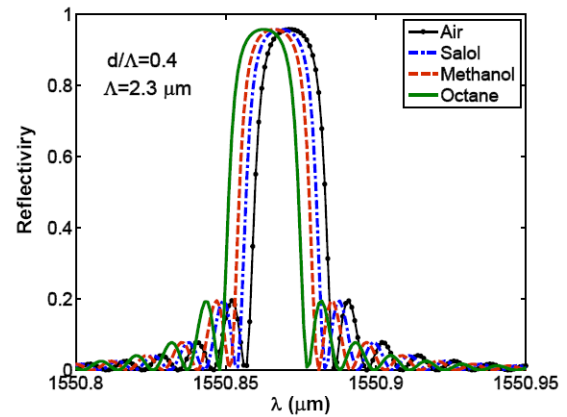


Figure 4. Computed power reflectivity spectra when different liquids are inserted in the PCF air-holes.

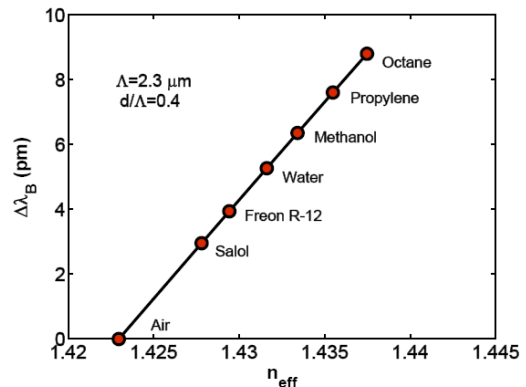


Figure 5. Sensitivity characteristic curve showing the simulated changes in Bragg wavelength versus the effective RI.

Figure 5 shows the relative Bragg wavelength shift as a function of the fluid RI, where the reference wavelength is taken the Bragg wavelength for air-filled PCF holes. It is worthy to note that the Bragg shift, although relatively weak, is linear and hence, the device is extremely suitable for sensor applications. Moreover, Fig. 6 shows the linear dependence of the relative bandwidth on the effective RI.

Finally, we explore the dependence of relative Bragg shift on the ratio d/Λ , for a PCF grating with air-filled holes. As it is seen in Fig. 7, the relative Bragg shift increase as the hole diameter increases.

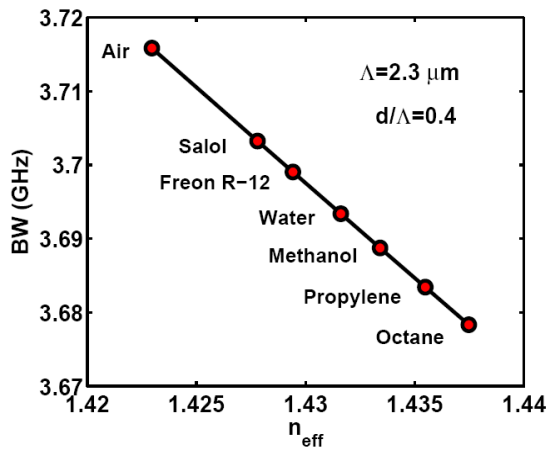


Figure 6. Bandwidth of the PCF Bragg grating versus the effective RI

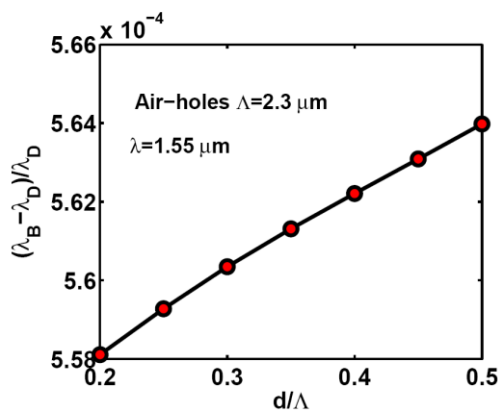


Figure 7. Relative Bragg shift of the PCF grating versus air-hole diameter.

4. CONCLUSION

The characteristics of PCF Bragg gratings are simulated utilizing a full-vectorial multipole method combined with coupled mode theory. For the design wavelength of $\lambda_D \sim 1.55 \mu\text{m}$, the reflectivity spectrum has been explored by filling the holes of PCF with different fluids. The shift in both the Bragg wavelength and bandwidth is found to be linear and hence, the device can be used as fluidic sensor or as tunable filter

References

- [1] O. Frazão et. al., Optical Sensing with Photonic Crystal Fibers, *Laser and Photonics Reviews*, Vol. 2 (6), 2008, pp. 449-459.
- [2] G. Kliros, K. Papageorgiou, Refractometric Optical Sensor based on Tapered Photonic Crystal Waveguide, *Journal of Optoelectronics and Advanced Materials*, Vol.12 (7), 2010, pp. 1530-1533.
- [3] G. Kliros, K. Papageorgiou, FDTD Modeling of Refractometric Optical Sensors based on Quasi-1D Photonic Crystals, *Journal of Applied Electromagnetism (JAE)*, Vol.12 (3), 2010, pp. 39-45.
- [4] A. Othonos, K. Kalli, *Fiber Bragg Gratings: Fundamentals and Applications in Telecommunications and Sensing*. Norwood, MA: Artech House, 1999.
- [5] T.P. White et. al., Multipole method for microstructured optical fibers, *J. Opt. Soc. Am. B*, Vol. 19 (10), 2002, pp. 2322-2340.